







Communication

Gold as Pollution Tracer in Holocene Sediments of the Doñana National Park, the Largest Biological Reserve in Europe

Verónica Romero ¹, Francisco Ruiz ^{1,2,*}, María Luz González-Regalado ¹, María Isabel Carretero ³, Manuel Pozo ⁴, Guadalupe Monge ⁴, Luis Miguel Cáceres ¹, Joaquín Rodríguez Vidal ^{1,5}, Manuel Abad ⁶, Tatiana Izquierdo ⁶, Antonio Toscano ¹, Paula Gómez ¹ and Gabriel Gómez ¹

¹ Departamento de Ciencias de la Tierra, Universidad de Huelva, Avda. 3 de Marzo, s/n, 21720 Huelva, Spain; vero.ra93@gmail.com (V.R.); montero@uhu.es (M.L.G.-R.); mcaceres@uhu.es (L.M.C.); jrvidal@uhu.es (J.R.V.); antonio.toscano@dgyp.uhu.es (A.T.); paula.gomezgutierrez@hotmail.com (P.G.); ggomezalvarez@yahoo.es (G.G.)

² Centro de Investigación en Patrimonio Histórico, Cultural y Natural, Universidad de Huelva, Campus Universitario de El Carmen, 21720 Huelva, Spain

³ Departamento de Cristalografía, Mineralogía y Química Agrícola, Universidad de Sevilla, C/Profesor García González, s/n, 41012 Sevilla, Spain; carre@us.es

⁴ Departamento de Geología y Geoquímica, Universidad Autónoma de Madrid, 28049 Madrid, Spain; manuel.pozo@uam.es (M.P.); gmonge@us.es (G.M.)

⁵ Gibraltar Natural Museum, Parson's Lodge Battery, Rosia Rd, Gibraltar GX11 1AA, Gibraltar

⁶ Departamento de Biología y Geología, Física y Química Inorgánica, Escuela Superior de Ciencias Experimentales y Tecnología (ESCET), Universidad Rey Juan Carlos, c/Tulipán s/n, 28933 Móstoles, Spain; manuel.abad@urjc.es (M.A.); tatiana.izquierdo@urjc.es (T.I.)

* Correspondence: ruizmu@uhu.es

Abstract

Estuaries are excellent containers for the prehistorical and historical pollution that develops in their river basins. This paper studies the Au contents obtained by inductively coupled plasma spectrometry of two cores extracted from the Doñana National Park (Guadalquivir Estuary, SW Spain). Concentrations of this precious metal have been associated with the different prehistoric and historical stages of exploitation of the Iberian Pyritic Belt. The three detected peaks correspond to the first mining operations in the area around the park, the first systematic Tartessian mining and strong exploitation during the Roman period. Consequently, Au is an appropriate marker of the contamination phases prior to its current extraordinary biological diversity.

Keywords: gold; prehistoric–historic pollution; estuary; SW Spain



Academic Editor: Giovanni Martinelli

Received: 25 May 2025

Revised: 24 July 2025

Accepted: 28 July 2025

Published: 30 July 2025

Citation: Romero, V.; Ruiz, F.; González-Regalado, M.L.; Carretero, M.I.; Pozo, M.; Monge, G.; Cáceres, L.M.; Vidal, J.R.; Abad, M.; Izquierdo, T.; et al. Gold as Pollution Tracer in Holocene Sediments of the Doñana National Park, the Largest Biological Reserve in Europe. *Minerals* **2025**, *15*, 801. <https://doi.org/10.3390/min15080801>

Copyright: © 2025 by the authors. Licensee MDPI, Basel, Switzerland. This article is an open access article distributed under the terms and conditions of the Creative Commons Attribution (CC BY) license (<https://creativecommons.org/licenses/by/4.0/>).

1. Introduction

In recent years, research on pollution in coastal environments such as estuaries, deltas, bays or lagoons has proliferated. A substantial part has focused on the determination of past episodes caused by mining operations, industrial effluents, urban waste or agricultural residues. For this purpose, geochemical analysis of sediment cores is frequently used, in which the concentrations of certain metals (e.g., Cu, Pb, Zn) allow characterization of these pollution events in coordination with radiometric dating [1–4].

The Iberian Pyritic Belt (SW Spain) (Figure 1: IPB) is one of the most important metallogenic provinces in Europe, with numerous giant deposits of polymetallic sulfides, whose extraction began some 5000 years ago [5,6]. These deposits are also one of the most important sources of Au in the Iberian Peninsula, especially in areas rich in Zn and gossans, within arsenopyrite or, in general, in all pyritic ores, although in low proportions. Known

concentrations of Au in massive sulfides range from 0.01 to 60 mg kg⁻¹, with Au found in most cases as electrum and alloys, with notable contents in Ag and Hg [7–9].

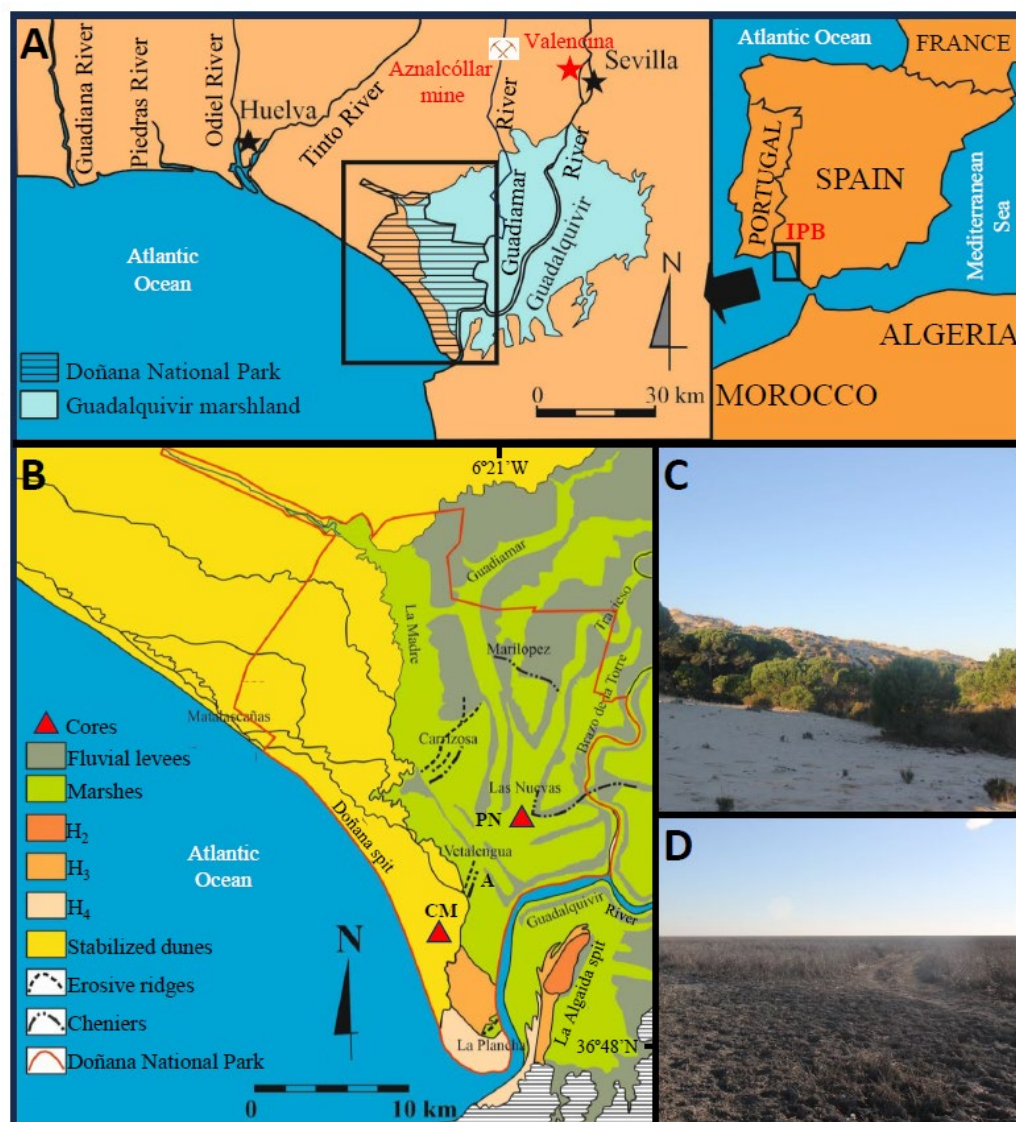


Figure 1. (A) Location of the Doñana National Park; (B) synthetic geomorphological map of Doñana National Park and adjacent areas; (C) partial view of the Doñana spit; (D) partial view of the Guadalquivir marshlands.

The study of numerous sediment cores in the adjoining estuaries has differentiated four Holocene peaks of metallic pollution, based mainly on the concentrations of Ag, Cu, Ni, Pb or Zn. One natural acid rock drainage event is related to the MIS-1 transgression (~6500 cal. yr BP), followed by three peaks of anthropogenic origin from early mining (~5000–4500 yr BP), the Roman period (~2100–1800 yr BP) and intensive mining together with industrial wastes between 1850 and 2000 [10–12]. However, this area was famous for its richness in silver during the Tartessian period (2900–2600 yr BP), with a subsequent decline in the silver trade with the Mediterranean peoples during the Turdetan period (2500–2200 yr BP) [13]. During these last periods, this metal was extracted in several mining sites such as Aznalcóllar (Figure 1A), associated with much lower concentrations of Au [14]. Consequently, it is reasonable to assume that any pollution episode in the Iberian Pyrite Belt would also lead to an increase in gold concentrations in the adjacent estuaries, although in much smaller quantities than the aforementioned metals.

This communication analyzes the Au content of two long sediment cores extracted from the Doñana National Park (SW Spain), the largest biological reserve in Europe. The aim is to test whether the temporal distribution of this precious metal can be used to identify past periods of pollution in this area. This distribution is compared with that of other elements frequently used as pollution markers.

2. Materials and Methods

2.1. Study Area

Doñana National Park (DNP) is located within the estuary of the Guadalquivir River (SW Iberian Peninsula) (Figure 1A). It is the largest biosphere reserve in Spain (542 km²) and is partially protected by an elongate sandy spit composed of stabilized dunes and ridges deposited during three phases of progradation (Figure 1B,C; H₂: 4200–2550 cal. yr BP; H₃: 2300–800 cal. yr BP; H₄: 500 cal. yr BP to the present) [15]. Most of the park is made up of flat marshes (Figure 1B–D) and fluvial levees, on which sandy and bioclastic ridges are deposited from the action of high-energy events [16].

DNP is connected to the Aznalcóllar mines through the Guadiamar River, a tributary of the Guadalquivir River (Figure 1A), and consequently, the millenary mining operations in this sector of the Iberian Pyrite Belt may have had an impact on the geochemistry of its Holocene sediments. This connection became evident on 25 April 1998, when the rupture of a settling pond at the Aznalcóllar mine caused an ecological disaster in the Guadiamar River and only the construction of dikes prevented the entry of sludge highly contaminated by heavy metals into the park [17].

2.2. Cores: Paleoenvironmental Reconstruction

Two long cores (Figure 1B: PN and CM) were drilled by the Spanish Geological and Mining Institute (IGME) in the southwestern part of DNP, and previous multidisciplinary studies have reconstructed their paleoenvironmental evolution. Core PN (Figure 2A) was located close to the so-called ‘Palacio de Las Nuevas’, and its upper 27.5 m are composed of (i) bioclastic sandy silts (27.5–26 m depth), deposited during the MIS-1 transgression; (ii) lagoonal muds (26–11.4 m depth) with numerous fragments and carapaces of molluscs; (iii) a first tsunamigenic layer (11.4–9.3 m depth), characterized by a mixture of marine mollusks and brackish microfauna; (iv) a monotonous sequence of muds and silts (9.3–1.8 m depth) whose faunal content (macrofauna, ostracods, foraminifera, etc.) testifies to the transit from an open lagoon to a tidal channel; and (v) a second tsunamigenic layer (1.8–0 m depth) composed of silty sands and sandy silts with abundant disarticulated valves and fragments of bivalves, together with frequent carapaces of gastropods, brackish and marine ostracods and even planktonic foraminifera [18].

Core CM (Figure 1B) was extracted in the Doñana spit and a previous multidisciplinary study carried out its paleoenvironmental reconstruction [16]. Four sedimentary facies have been distinguished in the geological record of this core (Figure 2B): (i) grayish silts with abundant marine bivalves, gastropods and benthic foraminifera deposited in a lagoon inlet; (ii) greenish to grayish clays with abundant brackish hyaline and agglutinated benthic foraminifera typical of salt marshes and lagoon margins; (iii) a thick tsunamigenic layer (~3rd century BCE), with yellow sands from the erosion of the dune ridges that make up the Doñana spit; and (iv) yellow dune sands with cross stratification and absence of both macrofauna and microfauna.

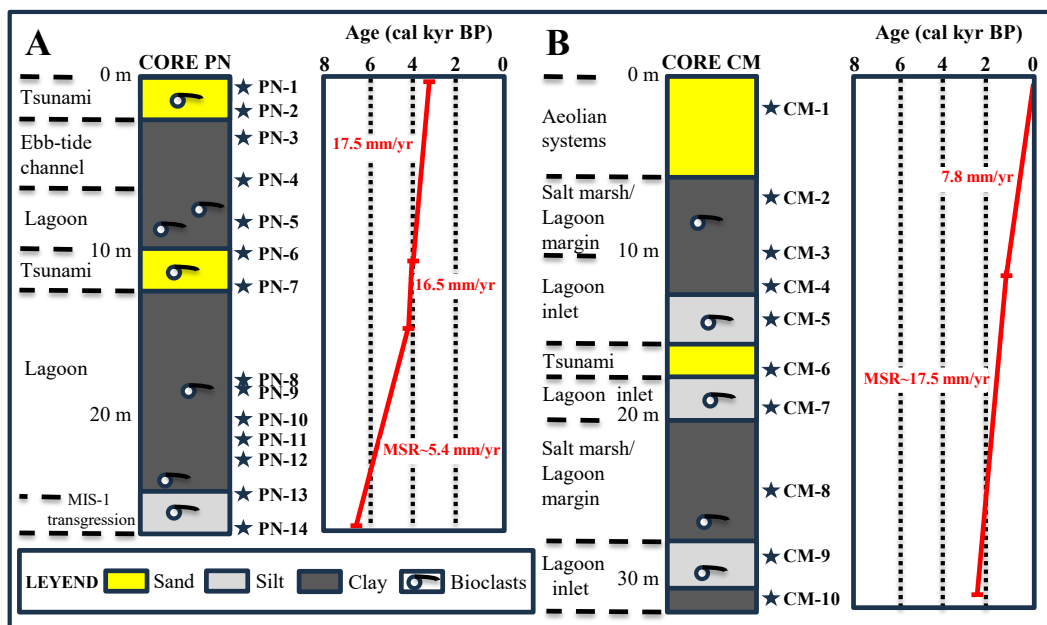


Figure 2. (A) Depth–age model of core PN; (B) depth–age model of core CM.

2.3. Sampling and Geochemical Analysis

Twenty-four samples (2 cm thick) were selected from the two cores (PN: PN-1 to PN-14; CM: CM-1 to CM-10). Selection and distribution of the samples are variable, linked to (i) the length of each core; (ii) the presence of different sedimentary facies; (iii) the definition of its limits; and (iv) the visual distribution of bioclasts. Consequently, the number of samples from each core depends on its geological features. This methodology has been used with fruitful results in other cores obtained in estuaries close to DNP [19].

At least one sample from each of these facies has been selected for geochemical study. These samples were stored in polyethylene bags until chemical analyses. These analyses were performed by Activation Laboratories (Ancaster, ON, Canada). Concentrations of Au were determined by inductively coupled plasma spectrometry, with calibration based on the analysis of over 30 international standard reference materials. The detection limit was $0.2 \mu\text{g kg}^{-1}$. The results were compared both directly and statistically with the concentrations of other usual tracers of pollution in the same samples obtained in previous investigations.

2.4. Dating

Six radiocarbon dates were obtained at Beta Analytic Laboratories (Miami, FL, USA) by AMS using samples of marine mollusk shells. These dates were calibrated using the Calib 8.2 program with the reservoir correction determined for this area [20]. A depth–age model was then produced for each core and the mean sedimentation rates (MSRs) were calculated for each period between two dates.

3. Results and Discussion

3.1. Dating and Depth-Age Models of Cores

The four dates obtained from the base to the top of the PN core range from the MIS-1 transgression (6.3–6.6 cal. kyr BP) to 3.2–3.6 cal. kyr BP (Table 1). The two tsunamigenic layers are similar in age (4–4.4 cal. kyr BP and 3.2–3.6 cal. kyr BP) to other tsunamigenic beds observed in short cores and trenches in the Doñana National Park, confirming the record of at least two high-energy events during the middle Holocene [21]. On the other hand, the geological record of the CM core spans approximately the last 2500 years. The wind-driven

tsunamigenic layer, located between 2500 years BP and 1600 years BP, corresponds to the tsunami that invaded this area during the third century BCE [22].

Table 1. ¹⁴C database of cores.

Core	Depth (m)	Laboratory Number	¹⁴ C Age Yr BP	Error	Age Cal Yr BP (2σ)
PN	0.3	B-228880	3550	40	3215–3580
	10.8	B-228881	4060	40	3845–4256
	14.1	B-228885	4200	40	4026–4433
	26.1	B-228882	6090	40	6270–6619
CM	11.7	B-228873	2030	40	1370–1714
	31	B-228876	2830	40	2349–2704

In the PN core (Figure 2A), the MSR is moderate (5.4 mm/yr), from ~6.4 cal. kyr BP to ~4.2 cal. kyr BP, and then increases markedly to ~3.4 cal. kyr BP (16.5–17.5 mm/yr). A similar rate has been obtained for the CM core between 2.5 cal. kyr BP and 1.5 cal. kyr BP (Figure 2B), decreasing markedly up to the present (7.8 mm/year). This indicates that the MSR was significantly higher in the outer areas of DNP than in its innermost sector (<5 mm/year) during this period [23].

3.2. Vertical Distribution of Au

Bioclastic silts and clays located at the base of the PN core (27.5–20 m depth; samples PN-14 to PN-10) do not exceed the detection limit (Figure 3A). This contrasts with the gold peak (6 μg kg⁻¹) detected in the lagoonal clays at a 19 m depth (sample PN-9) and the relatively high Au concentrations (4 μg kg⁻¹) until the tsunami that occurred between 3.8 and 4.2 cal kyr BP (samples PN-6 and PN-7). These concentrations do not exceed 2 μg kg⁻¹ in the uppermost six samples of this core, deposited over the next ~600 years.

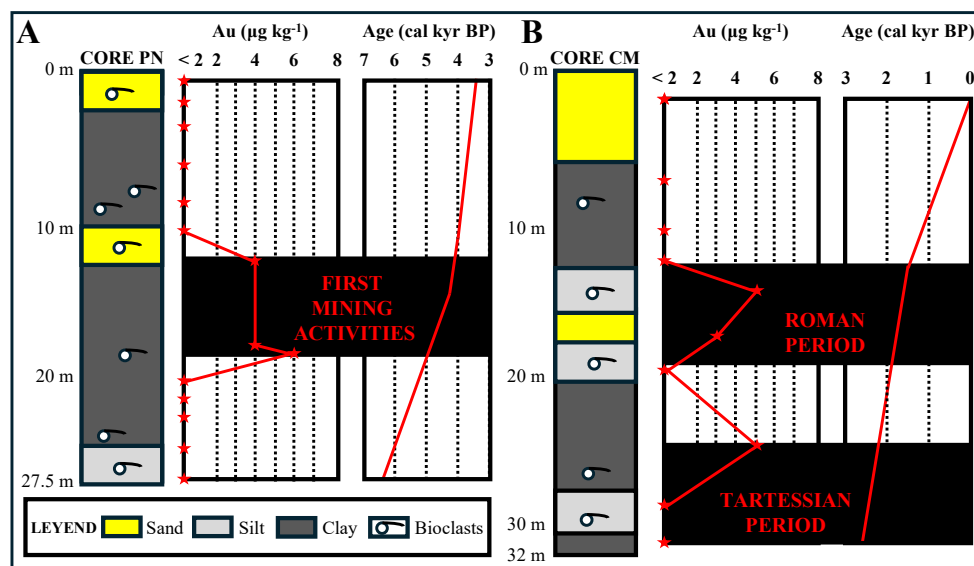


Figure 3. Cores logs with sampling, gold concentrations and pollution periods. (A) Core PN; (B) core CM. The stars represent the concentration of gold in each sample.

The lower samples of the CM core (Figure 3B; samples CM-10 and CM-9), deposited at the mouth of an old lagoon, also do not exceed the detection limit. A first peak (sample CM-8; 5 μg kg⁻¹) was detected in the clays that constituted the margins of this lagoon, followed by a decrease below detection limits until the third-century BCE tsunami. Gold concen-

trations increased because of this high-energy event (sample CM-6; $3 \mu\text{g kg}^{-1}$), which preceded a new peak (sample CM-5; $5 \mu\text{g kg}^{-1}$) located in the bioclastic silts deposited about ~2000 years ago at the mouth of the old lagoon.

3.3. Au as Prehistorical and Historical Pollution Tracer

A joint view of Au concentrations in both cores, together with historical data and paleoenvironmental reconstructions, defines different pollution episodes linked to anthropogenic actions during the last 7000 years in DNP. During the MIS-1 transgression (~6500 yr BP), the estuaries of the southwestern Iberian Peninsula were invaded by the sea, and in some of them (Figure 1A: Tinto River), there is a first pollution peak due to acid rock drainage resulting from the leaching of surface beds of the massive sulfide deposits of the IPB [11]. However, this episode is not reflected in the Holocene sediments of the southwestern DNP (core PN), probably because of its location near the mouth of an old lagoon and the possible tidal dilution of this natural pollution.

The Iberian Pyrite Belt is one of the oldest mining districts in the world, with more than 4500 years of history [24]. The start of mining is clearly reflected in the first Au peak detected in the lagoonal clays of PL core ($4\text{--}6 \mu\text{g kg}^{-1}$), with an age of at least 4500 years BP (Figure 3A). During the third millennium BCE, mining was restricted to the exploitation of Cu minerals (azurite, malachite, cuprite, tenorite, chalcocite and covellite) extractable at the surface or at shallow depths [25,26]. The copper ores were processed in centers located near the margins of the lagoon, such as Valencina (Figure 1A), between 4.7 and 4.5 cal. kyr BP [25]. The palaeogeographical reconstruction of this area during this period (Figure 4) reflects the connection between these metallurgical centers and the location of the PN core, which would explain the first Au peak detected there.

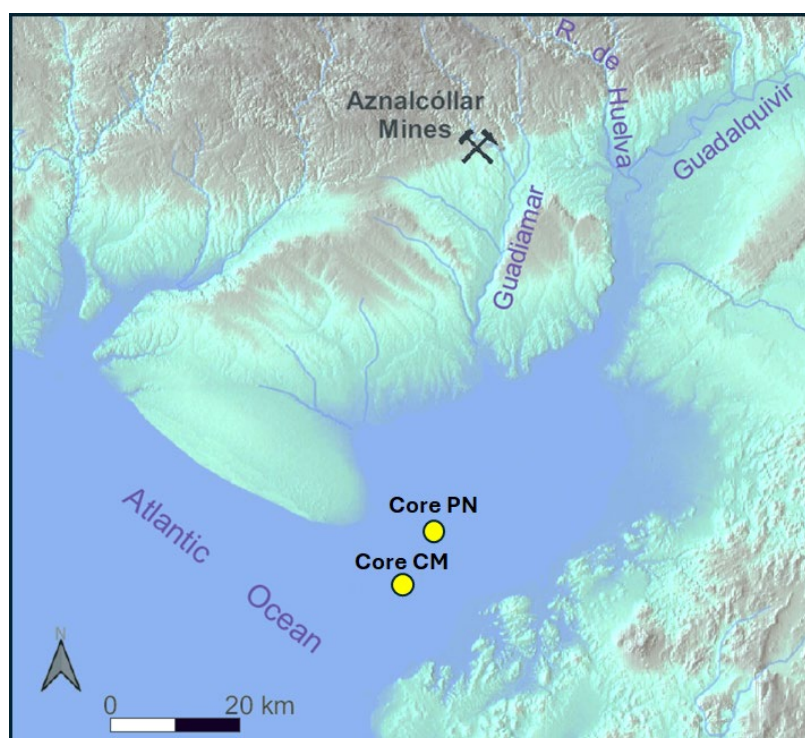


Figure 4. Palaeogeographical reconstruction of the Guadalquivir Estuary around 5000–4000 yr BP [27].

The first systematic exploitation of the IPB deposits took place during the Tartessian period, developed in the southwest of the Iberian Peninsula between 2900 yr BP and 2600 yr BP. There are no written sources for this period and their quotations come from

Greco-Latin authors. Different historical sources make reference to Tartessos, such as the Bible, Herodotus (5th century BC), Strabo (1st century BC–1st century AD) or Avieno (4th century AD) [28]. A substantial part of the research on this civilization has focused on its importance as a mining emporium and source of minerals (especially copper, silver and gold) for the peoples of the eastern Mediterranean, such as the Phoenicians. This mining reactivation is probably reflected in the first Au peak of the CM core ($3 \mu\text{g kg}^{-1}$), which would coincide with the splendor of silver metallurgy in settlements located in the Aznalcóllar area, such as Los Castrejones or the Aznalcóllar castle [29].

Tartessian society underwent a major crisis around 2600–2500 yr BP [30]. The later pre-Roman period differs from it both culturally and linguistically, such that Strabo called the inhabitants of this area Turdetans [31,32]. The Turdetan period (~2500–2200 yr BP) was characterized by a remarkable mining decline [33], expressed in the CM core by Au contents below detection limits (sample CM-7).

The Roman mining boom in the IPB (2100–1800 yr BP) involved the extensive mining of the massive sulfide deposits in this area, with the extraction of some 20 Mt [24]. The Aznalcóllar mines were intensively exploited for the extraction of copper and silver, both in gossans and in primary mineralization. In addition, there were several metallurgical settlements where abundant iron, lead, silver, copper and copper–iron slags had been found [34]. This intense mining activity is reflected in the second Au peak in the CM core (Figure 3B: up to $5 \mu\text{g kg}^{-1}$), as well as in numerous cores extracted in the estuary of the Tinto and Odiel rivers [10–12]. The subsequent clogging of the lagoon, coupled with a subsequent remarkable mining decline from the fall of the Roman Empire to the new intensive mining of the IPB during the 19th and 20th centuries and the progressive shrinkage of the Doñana shaft, is reflected in the Au concentrations below $2 \mu\text{g kg}^{-1}$ in the upper part of this core. It should be noted that gold contamination continues for a short period of time, even after each prehistoric or historical episode of contamination (Figure 3A,B), possibly reflecting the role of surface runoff on abandoned tailings piles.

3.4. Au vs. Other Pollution Tracers

Table 2 shows the concentrations of Au and other elements frequently used as pollution tracers in the studied cores [12,22]. This table allows us to compare their variations in relation to the main pollution episodes over the last 5000 years in DNP. The former mining activities (~4500 yr BP) are reflected in the increase in precious metals (Au, Ag) in the CM core, while the other pollution tracers do not show significant increases. However, peaks of Cu, Pb and Zn have been found in estuaries close to DNP in sediments of this age [11]. This may be due to (i) differences between mined ores; (ii) different palaeogeography; or (iii) differential fluvial dynamics.

In the PN core, both Tartessian and Roman mining caused a substantial increase in all the elements analyzed in relation to the underlying sediments, with values six to seven times higher in their concentrations. These periods witnessed a systematic exploitation of the Iberian Pyrite Belt, and all the estuaries located between DNP and the current border with Portugal and even the adjacent marine shelf were contaminated by Cu, Pb and Zn [6,35]. However, gold is not analyzed as a possible tracer of contamination in these investigations.

The bivariate statistical analysis between gold and these metals does not yield significant linear correlations for the six samples with gold values above the detection limit ($r = 0.47$ for Cu; $r = 0.62$ for Pb; $r = 0.43$ for Zn). If the mean value of the detection limit is taken for the remaining samples ($\text{Au} = 1 \mu\text{g kg}^{-1}$), the correlations are practically zero ($r = 0.07$ for Cu; $r = 0.02$ for Pb; $r = 0.01$ for Zn). Consequently, there is no statistical correlation between Au values and other possible tracers of contamination in these cores, although

their values increase simultaneously during certain pollution periods. This may be partly due to the very low concentrations of Au concerning the rest of the elements analyzed.

Table 2. Comparison between Au concentrations (in $\mu\text{g kg}^{-1}$) and other pollution tracers (in mg kg^{-1}).

Core	Sample/Element	Au	Ag	Cu	Pb	Zn
CM	CM-1	<2	<0.3	4	5	9
	CM-2	<2	0.3	33	41	81
	CM-3	<2	<0.3	29	37	75
	CM-4	<2	<0.3	30	35	71
	CM-5: Roman pollution	5	<0.3	19	25	46
	CM-6	3	<0.3	5	7	7
	CM-7	<2	<0.3	12	21	28
	CM-8: Tartessian pollution	5	0.6	46	46	74
	CM-9	<2	0.4	5	7	12
	CM-10	<2	<0.3	3	6	9
PN	PN-1: Tsunami	<2	<0.3	22	21	61
	PN-2: Tsunami	<2	0.3	24	18	68
	PN-3	<2	0.4	37	54	79
	PN-4	<2	0.4	32	46	75
	PN-5	<2	0.4	27	32	62
	PN-6: Tsunami	<2	<0.3	28	15	61
	PN-7: Tsunami	4	<0.3	14	12	58
	PN-8	4	<0.3	22	16	66
	PN-9: First mining activities	6	0.4	18	14	60
	PN-10	<2	<0.3	20	10	68
	PN-11	<2	<0.3	20	12	62
	PN-12	<2	<0.3	18	14	59
	PN-13: MIS-1 transgression	<2	<0.3	19	13	62
	PN-14: MIS-1 transgression	<2	<0.3	18	10	56

4. Conclusions

The geochemical analysis of two cores obtained in DNP attests to the applicability of gold as a tracer of contamination derived from the Iberian Pyritic Belt in the Guadalquivir River Estuary. The temporal evolution of the Au concentrations is consistent with the proto-historic and historical data on the development of the Aznalcóllar mines, its surroundings and the people who inhabited the area around DNP more than 4000 years ago. The three detected peaks correspond to the first mining activities, a first phase of systematic Tartessian mining and strong exploitation during the Roman period. The content of precious metals (Au, Ag) detects the earliest mining activities in the Iberian Pyrite Belt, while both these elements and others (Cu, Pb, Zn) increased significantly during the Tartessian and Roman periods. However, there is no significant statistical correlation between gold and other metals, although all of them increased both during periods of pollution and during a brief interval after them.

Author Contributions: V.R., F.R., M.L.G.-R., M.I.C., M.P., G.M., L.M.C., J.R.V., M.A., T.I., A.T., P.G. and G.G. have participated in all stages of the paper. All authors have read and agreed to the published version of the manuscript.

Funding: This research was supported by the project ‘El arco atlántico del sudoeste hispano desde la protohistoria hasta la Tardoantigüedad: Evolución geomorfológica, ocupación litoral y sistemas portuarios’ (PID2022-142778NB-I00), funded by the Ministry of Science and Innovation of Spain. This work was also funded by the research groups RNM-238 and RNM-293 (University of Huelva). It is a contribution to the Centre for Research in Historical, Cultural and Natural Heritage of the University of Huelva.

Data Availability Statement: Data are available upon request to the corresponding author.

Conflicts of Interest: The authors declare no conflicts of interest.

References

1. Ghanem, A.; Nada, A.; Abu-Zeid, H.; Madcour, W.; Shetaia, S.A.; Imam, N. Historical trends of heavy metals applying radiocarbon dating and neutron activation analysis (NAA) in sediment cores, Burullus Lagoon, Egypt. *Environ. Sci. Pollut. Res.* **2024**, *31*, 43633–43658. [[CrossRef](#)]
2. Zhang, S.; Li, Q.; Zou, Y.; Liu, B.; Yang, J.; Zheng, H.; Liu, G. Using isotopic lead and strontium in sediments to trace natural and anthropogenic sources in the Bohai Sea. *Sci. Rep.* **2024**, *14*, 30267. [[CrossRef](#)]
3. Nagarajan, A.; Dharmalingam, S.N.; Jeyasingh, V.; Jayaseelan, C.; Vijayaprabakaran, K. Heavy metals in core sediments from the western Bay of Bengal: Implications on historical pollution, eco-environmental risks, and potential sources. *Anthr. Coasts* **2024**, *7*, 26. [[CrossRef](#)]
4. Ahmad, M.Z.; Singh, P. Geochemistry of core sediments from Cauvery delta South-East India: Inferences on weathering and paleo-redox conditions. *Quaternaire* **2023**, *34*, 18588.
5. Tornos, F.; López, E.; Sánchez, F.J. The Iberian Pyrite Belt. In *Contextos Geológicos Españoles: Una Aproximación al Patrimonio Geológico de Relevancia Internacional*; García-Cortés, A., Ed.; Instituto Geológico y Minero de España: Madrid, Spain, 2008; pp. 56–64.
6. Delgado, J.; Boski, T.; Nieto, J.; Pereira, L.; Moura, D.; Gomes, A.; Sousa, C.; García-Tenorio, R. Sea-level rise and anthropogenic activities recorded in the late Pleistocene/Holocene sedimentary infill of the Guadiana Estuary (SW Iberia). *Quat. Sci. Rev.* **2012**, *33*, 121–141. [[CrossRef](#)]
7. Leistel, J.M.; Marcoux, E.; Deschamps, Y.; Joubert, M. Antithetic behaviour of gold in the volcanogenic massive sulphide deposits of the Iberian Pyrite Belt. *Miner. Depos.* **1997**, *33*, 82–97. [[CrossRef](#)]
8. Velasco, F. El oro asociado a los sulfuros masivos de la Faja Pirítica Ibérica. *Macla* **2014**, *19*, 1.
9. Yesares, L.; Ruiz de Almodóvar, G.; Sáez, R.; Proenza, J.A.; Pons, J.M. Mineralizaciones de oro en los sulfuros masivos de la Faja Pirítica Ibérica. *Macla* **2019**, *24*, 121–122.
10. Cáceres, L.M.; Ruiz, F.; Bermejo, J.; Fernández, L.; González-Regalado, M.L.; Rodríguez Vidal, J.; Abad, M.; Izquierdo, T.; Toscano, A.; Gómez, P.; et al. Sediments as sentinels of pollution episodes in the middle estuary of the Tinto River (SW Spain). *Minerals* **2023**, *7*, 95. [[CrossRef](#)]
11. Davis, R.A.; Welty, A.T.; Borrego, J.; Morales, J.A.; Pendón, J.G.; Ryan, J.G. Rio Tinto estuary (Spain): 5000 years of pollution. *Environ. Geol.* **2000**, *39*, 1107–1119. [[CrossRef](#)]
12. Ruiz, F.; Rodríguez Vidal, J.; Cáceres, L.M.; Olías, M.; González-Regalado, M.L.; Campos, J.M.; Bermejo, J.; Abad, M.; Izquierdo, T.; Carretero, M.I.; et al. Silver and copper as pollution tracers in Neogene to Holocene estuarine sediments from southwestern Spain. *Mar. Pollut. Bull.* **2020**, *150*, 110704. [[CrossRef](#)] [[PubMed](#)]
13. Fernández Jurado, J. Economía tartésica: Minería y metalurgia. *Huelva Hist.* **1986**, *1*, 149–170.
14. Escacena, J.L.; Feliu, M.J.; Izquierdo, R. El Cerro de La Albina y la metalurgia de la plata en Tartessos. *De Re Met. (Madr.) Rev. De La Soc. Española Para La Def. Del Patrim. Geológico Y Min.* **2010**, *14*, 35–51.
15. Dabrio, C.J.; Zazo, C.; Lario, J.; Goy, J.L.; Sierro, F.J.; Borja, F.; González, J.A.; Flores, J.A. Sequence stratigraphy of Holocene incised-valley fills and coastal evolution in the Gulf of Cádiz (southern Spain). *Geol. En Mijnb.* **1998**, *77*, 263–281. [[CrossRef](#)]
16. Rodríguez-Ramírez, A.; Villarías-Robles, J.J.R.; Pérez-Asensio, J.N.; Santos, A.; Morales, J.A.; Celestino-Pérez, S.; León, A.; Santos-Arévalo, F.J. Geomorphological record of extreme wave events during Roman times in the Guadalquivir estuary (Gulf of Cadiz, SW Spain): An archaeological and paleogeographical approach. *Geomorphology* **2016**, *261*, 103–118. [[CrossRef](#)]
17. Ayala-Carcedo, F.J. La rotura de la balsa de residuos mineros de Aznalcóllar (España) de 1998 y el desastre ecológico consecuente del río Guadiamar: Causas, efectos y lecciones. *Bol. Geol. Min.* **2004**, *115*, 711–738.
18. Pozo, M.; Ruiz, F.; Carretero, M.I.; Rodríguez Vidal, J.; Cáceres, L.M.; Abad, M.; González-Regalado, M.L. Mineralogical assemblages, geochemistry and fossil associations of Pleistocene-Holocene complex siliciclastic deposits from the Southwestern Donana National Park (SW Spain): A palaeoenvironmental approach. *Sediment. Geol.* **2010**, *225*, 1–18. [[CrossRef](#)]
19. Prudêncio, M.I.; Ruiz, F.; Marques, R.; Dias, M.I.; Vidal, J.R.; Rodrigues, A.L.; Cáceres, L.M.; González-Regalado, M.L.; Muñoz, J.M.; Pozo, M.; et al. REE Geochemistry of Neogene–Holocene Sediments of La Fontanilla Cove (Tinto Estuary, SW Spain). *Minerals* **2022**, *12*, 417. [[CrossRef](#)]
20. Martins, J.M.M.; Soares, A.M.M. Marine radiocarbon reservoir effect in southern Atlantic Iberian coast. *Radiocarbon* **2013**, *55*, 1123–1134. [[CrossRef](#)]
21. Rodríguez-Ramírez, A.; Pérez-Asensio, J.N.; Santos, A.; Jiménez-Moreno, G.; Villarías-Robles, J.J.R.; Mayoral, E.; Celestino-Pérez, S.; Cerrillo-Cuenca, E.; López-Sáez, J.A.; León, A.; et al. Atlantic extreme wave events during the last four millennia in the Guadalquivir estuary, SW Spain. *Quat. Res.* **2015**, *83*, 24–40.

22. González-Regalado, M.L.; Monge, G.; Carretero, M.I.; Pozo, M.; Rodríguez-Vidal, J.; Cáceres, L.M.; Abad, M.; Campos, J.M.; Bermejo, J.; Tosquella, J.; et al. Imprints of historical pollution and the 218–60 BCE tsunamigenic period in southwestern Spain. *Rev. Mex. Cienc. Geol.* **2020**, *37*, 89–97. [[CrossRef](#)]
23. Lario, J.; Zazo, C.; Goy, J.L.; Dabrio, C.J.; Borja, F.; Silva, P.G.; Sierro, F.; González, A.; Soler, V.; Yll, E. Changes in sedimentation trends in SW Iberia Holocene estuaries (Spain). *Quat. Int.* **2002**, *93–94*, 171–176. [[CrossRef](#)]
24. Tornos, F. La geología y metalogenia de la Faja Pirítica Ibérica. *Macla* **2008**, *10*, 13–23.
25. Nocete, F.; Queipo, G.; Sáez, R.; Nieto, J.M.; Inacio, N.; Bayona, M.R.; Peramo, A.; Cruz-Auñón, R. Specialised copper industry in the political centres of the Guadalquivir Valley during the Third Millennium BC: The smelting quarter of Valencina de la Concepción, Sevilla, Spain (2750–2500 BC). *J. Archaeol. Sci.* **2008**, *35*, 717–732. [[CrossRef](#)]
26. Pérez Macías, J.A.; Delgado Domínguez, A. Ingeniería minera antigua y medieval en el suroeste ibérico. *Boletín Geológico Y Min.* **2011**, *122*, 3–16.
27. Cáceres, L.M.; Donaire, T.; Ramírez-Cruzado, S.; Vargas, J.M.; Muñoz, F.; Martín, M.; Rodríguez Vidal, J.; Ruiz, F.; García Sanjuán, L. From the Mountain and the Sea: Provenance of the Stones of the Prehistoric La Pastora Tholos (Valencina de la Concepción, Seville, Spain). *Minerals* **2024**, *14*, 194. [[CrossRef](#)]
28. Alvarez, B.C. La civilización tartésica. *Hist. Digit.* **2016**, *16*, 98–135.
29. Pérez Macías, J.A. Las minas de Tarteso. In *Tarteso. El Emporio del Metal*; Alvar, J., Campos, J.M., Eds.; Archaeopress Publishing Ltd.: Córdoba, Spain, 2013; pp. 449–472.
30. Ferrer, E.; García, F.J. La crisis de Tarteso y el problema del siglo V a.C. en el ámbito geográfico turdetano. *Anales Arqueol. Cordob.* **2019**, *30*, 51–76.
31. Carrasco, J.L.E. Indicadores étnicos en la Andalucía prerromana. *Spal* **1992**, *1*, 321–343.
32. Strabo. *Geografía. Libros III–IV*; Biblioteca Clásica de Gredos: Madrid, Spain, 1992; Volume 169.
33. Pérez Macías, J.A. Pico del Oro (Tharsis, Huelva). Contraargumentos sobre la crisis metalúrgica tartésica. *Huelva Hist.* **1999**, *7*, 71–98.
34. Amores, F.; García, E.; Garrido, P.; Hunt, M.A.; Vázquez, J.; Rodríguez, J. Los paisajes históricos del Valle del Guadiamar (Sevilla): La minería y la metalurgia en el extremo oriental del Cinturón Ibérico de Piritas. *Cuad. De Prehist. Y Arqueol. De La Univ. De Granada* **2014**, *24*, 203–237. [[CrossRef](#)]
35. Mil-Homens, M.; Vale, C.; Naughton, F.; Brito, P.; Drago, T.; Anes, B.; Raimundo, J.; Schmidt, S.; Caetano, M. Footprint of roman and modern mining activities in a sediment core from the southwestern Iberian Atlantic shelf. *Sci. Total Environ.* **2016**, *571*, 1211–1221. [[CrossRef](#)] [[PubMed](#)]

Disclaimer/Publisher’s Note: The statements, opinions and data contained in all publications are solely those of the individual author(s) and contributor(s) and not of MDPI and/or the editor(s). MDPI and/or the editor(s) disclaim responsibility for any injury to people or property resulting from any ideas, methods, instructions or products referred to in the content.